J Solid State Electrochem (2005) 9: 106–113
DOI 10.1007/s10008-004-0558-1

ORIGINAL PAPER

U. Lavrenčič Štangar · B. Orel · J. Vince
V. Jovanovski · H. Spreizer · A. Šurca Vuk · S. Hočevar

Silicotungstic acid/organically modified silane proton-conducting membranes

Received: 24 October 2003 / Accepted: 29 March 2004 / Published online: 3 August 2004

Abstract Proton-conducting gels and membranes were made from an organically modified silane incorporating a heteropoly acid, i.e. silicotungstic acid. The ORMOSIL host was generated from a bis end-capped triethoxysilane chemically bonded via the urea bridges to (1) a long poly(propylene glycol) chain or (2) a long poly(dimethylsiloxane) chain. The heteropolyacid acted simultaneously as a source of mobile protons and as a catalyst, initiating the hydrolysis/condensation reactions of the sol–gel composite. In addition to the bis end-capped triethoxysilane network former, different alkoxysilanes were tested as network modifiers to optimize the gelation time, mechanical properties, ionic conductivity and the retention of the heteropolyacid during soaking of the membranes in water. Among alkoxysilane modifiers the most promising results were given by perfluorooctyltriethoxysilane and phenyltriethoxysilane. The conductivity of the membranes was up to 10^{-2}–10^{-1} S cm^{-1} at elevated temperatures and saturated humidity conditions. Fourier transform IR attenuated total reflection spectroscopy was used to follow the gelation of the samples and, in parallel to thermogravimetric/differential scanning calorimetry measurements, also the thermal stability of the membranes.

Keywords Proton-conducting membranes · Sol–gel · Silicotungstic acid · Organically modified silanes · Poly(dimethylsiloxane)

Introduction

In the light of efforts to use fossil fuels more efficiently and in future to replace them with renewable energy sources that have negligible pollutant emissions, fuel cells represent a growing and important field of research. Among them, the polymer electrolyte membrane fuel cell (PEMFC) has attracted considerable interest because of its high efficiency and convenient operating temperature. This type of fuel cell uses either pure hydrogen as fuel or hydrogen derived from available fossil fuels or renewables. In the search for renewable energy sources as alternatives to fossil fuels alcohols, especially methanol, represent viable options. They can be used as an energy vector for long-distance transportation and for centralized hydrogen production at the place of demand, using a similar infrastructure as today's oil economy. They can also be used for the on-board production of hydrogen in vehicles using autothermal reforming and several downstream processes to obtain more or less pure hydrogen for fuel-cell-based electric traction. They can, moreover, also be used as fuels in so-called direct methanol fuel cells (DMFC). The latter option seems to be the most elegant since it avoids all intermediate chemical processes for pure hydrogen production.

To make fuel cells really competitive for mass production and market penetration in certain niches such as stationary use in distributed power generation or mobile use in vehicle traction, efficient membranes need to be developed for PEMFCs with a lower cost than the perfluorosulfonic Nafion-like polymer membranes mostly used today. These latter membranes exhibit high proton conductivity and chemical stability, but, in addition to their high cost, especially in fuel cell production for vehicle applications, they are insufficiently stable for intermediate temperature operation above 363 K, which is desirable in vehicle traction applications of PEMFCs.

The membrane itself should be a good proton conductor, an electrical insulator and a separator of the reactant gases or liquids (fuel and oxygen); it therefore plays a key role in low-temperature fuel cells like PEMFCs and DMFCs. In recent years many contributions have appeared in the literature dealing with alternative low-cost membranes like sulfonated aromatic polymer membranes [1, 2, 3, 4, 5], complexes of basic

U. Lavrenčič Štangar · B. Orel (✉) · J. Vince · V. Jovanovski
H. Spreizer · A. Šurca Vuk · S. Hočevar
National Institute of Chemistry, Hajdrihova 19,
1000 Ljubljana, Slovenia
E-mail: boris.orel@ki.si

polymers with strong acids [2] such as poly(vinyl alcohol)/ phosphotungstic acid [6], or—the most relevant to this work—silica-based nanocomposite membranes [7, 8, 9, 10, 11, 12, 13, 14, 15, 16, 17, 18, 19, 20, 21, 22]. Honma and coworkers recently published a number of papers [10, 11, 12, 13, 14, 15, 16, 17] describing heteropolyacid (HPA)/silica nanocomposite membranes, made by the sol–gel procedure. Using this technique, the silica host was derived from simple tetraalkoxysilanes [7, 8, 18] or bis end-capped trialkoxysilanes with various bridging groups such as polyethers [10, 11, 12, 13, 15, 16, 19, 20, 21], alkylenes [13, 14, 16, 17] and aromatics [13, 16]. Good thermal stability and proton conductivities of up to around 10^{-2} S cm^{-1} (application level) were reported for HPA/silica membranes.

In the present work, organically modified silane (ORMOSIL) proton-conducting membranes were made from triethoxysilanes (organically modified with various bridging and pendant groups), silicotungstic acid (SiWA) and ethanol as a solvent, deliberately avoiding the addition of water. The ORMOSIL host was generated from isocyanatopropyltriethoxysilane (ICS) and diaminopropylpoly(dimethylsiloxane) ($M_r = 900$–$1{,}000$) giving an ICS–poly(dimethylsiloxane) (PDMS) sol–gel precursor consisting of a bis end-capped triethoxysilane bonded via the urea groups to a PDMS chain.

The use of ICS–PDMS represents a step forward in developing a complex amphiphilic precursor, different from similar precursors used so far by Honma and coworkers [10, 11, 12, 13, 14, 15, 16, 17]. It combines the protonating ability of the urea groups with the enhanced hydrophobicity of the PDMS chains in the same precursor.

To further work out the idea of having an amphiphilic host for the mobile proton species, we made and tested similar precursors used already in our laboratory and in others [15, 16, 19, 20, 21], i.e. bis end-capped propyltriethoxysilane bonded via the urea groups to a long ($M_r \sim 4{,}000$) poly(propylene glycol) (PPG) chain. We combined an ICS–PPG network former with single-capped trialkoxysilanes having phenyl (FTES) and perfluorooctyl (PFOTES) pendant groups imparting the hydrophobicity of the corresponding precursor mixtures. Another reason for adding single-capped hydrophobic FTES and PFTOES precursors to ICS–PDMS and ICS–PPG was to increase the gelling time of the latter when a large amount of SiWA was added to the precursor solution. This made it possible to compare the properties (proton conductivity, retention of SiWA at saturated humidity conditions, thermal stability) of ICS–PPG/PFOTES membranes (membrane A) with ICS–PDMS (membrane B) prepared without hydrophobic network modifiers (i.e. FTES or PFOTES), and led us finally to make and test a membrane where a synergetic effect of the ICS–PPG, ICS–PDMS and PFOTES components (membrane C) was expected.

SiWA acts simultaneously as a source of protons and as an acid catalyst, initiating hydrolysis/condensation reactions of the sol–gel composite. The major contribution to proton conductivity is obtained from the presence of water incorporated in the corresponding hybrids through the addition of SiWA. Proton transport is assured by the degree of hydration of the membrane. It is believed that for both the Grotthuss and the vehicular mechanisms, the proton forms an ion adduct with a diffusible carrier molecule. If the carrier molecule is water, the proton forms oxonium ions in the electrolyte. Therefore without the presence of water and proton-bearing species conventional polymer membranes do not give a sufficiently high proton conductivity. If such membranes are to be used at elevated temperatures (over 363 K) in the presence of an aqueous medium, lowering of the water vapour pressure in the membrane is needed. This could be achieved by adding an inorganic water-retention component like silica to the nanocomposite membrane.

Fourier transform (FT) IR spectroscopic measurements using an attenuated total reflection (ATR) accessory were performed to follow the gelation process in the membranes and their thermal stability by recording time-dependent and temperature-dependent IR ATR spectra, respectively. Thermogravimetric analysis was additionally used to determine the temperature stability of the precursors and the final membranes. The proton conductivity of the as-synthesized membranes was calculated from the measured impedance in the autoclave cell at 100% relative humidity (RH) within the temperature interval between room temperature and 433 K.

Experimental

Preparation of the membranes

The basic materials and chemicals used for making the membranes are shown in Fig. 1. Network-former sol–gel precursors of the two types (ICS–PPG and ICS–PDMS) were synthesized according to the following procedures.

1. ICS–PPG4000 [19, 23]: 20 g poly(propylene glycol)bis(2-aminopropyl ether) ($M_r \sim 4{,}000$) (Aldrich) and 2.5 g ICS (ABCR) were mixed with 20 g tetrahydrofuran (THF) under reflux (338 K) for 6 h. THF was evaporated, resulting in a viscous precursor. Similarly, the unhydrolysed silicon precursor having a shorter polymer chain, ICS–PPG2000, was prepared from poly(propylene glycol)bis(2-aminopropyl ether) with a relative molecular weight of 2,000.
2. ICS–PDMS1000: 14 g aminopropyl-terminated PDMS ($M_r \sim 900$–$1{,}000$) (ABCR) and 7.3 g ICS (ABCR) were mixed with 20 g THF under reflux (338 K) for 48 h. THF was evaporated, resulting in a viscous colourless precursor. Termination of the acylation reaction was verified by FT-IR spectroscopy of the sample between NaCl windows. The characteristic band at 2,271 cm^{-1} belonging to the

Fig. 1 Sol–gel precursors and other chemicals used in the preparation of proton-conducting membranes: ICS-PPG, ICS-PDMS, PFOTES, FTES, Brij 56, SiWA, PWA (abbreviations are explained in text)

isocyanato group practically disappeared after 48-h reaction time.

The network-modifier precursors PFOTES and phenyltriethoxysilane (FTES) and HPAs were used as received (ABCR and Aldrich, respectively). SiWA contained 11.6% of water. To facilitate the preparation of homogeneous membranes from the ICS–PDMS1000 network-former precursor, polyoxyethylene(10) cetyl ether surfactant Brij 56 (Aldrich) was added. The optimized quantities of the components for the three typical membranes based on ICS–PPG (membrane A), ICS–PDMS (membrane B) or both network formers, ICS–PPG and ICS–PDMS (membrane C) were

1. Membrane A—0.5 g ICS–PPG4000, 0.34 g PFOTES, 0.69 g SiWA, 2.3 mL EtOH.
2. Membrane B—0.5 g ICS-PDMS1000, 0.26 g Brij 56, 0.41 g SiWA, 2.3 mL EtOH.
3. Membrane C—0.5 g ICS–PDMS1000, 0.33 g ICS–PPG4000, 0.033 g FTES, 0.60 g SiWA, 2.7 mL EtOH.

The sol–gel processing of proton-conducting ORMOSIL membranes is presented schematically in Table 1. The membranes were produced by casting a fresh sol in a Teflon dish (diameter 6–9 cm), where it gelled and solidified, usually within 24 h when ethanol completely evaporated. The membranes contained about 40 wt % of anhydrous SiWA. ICS–PPG based membranes are transparent and flexible, while ICS–PDMS1000 based membranes are white and become brittle with ageing. However, the latter type of membrane has other advantages (no swelling, based on qualitative observations, and better retention of SiWA in boiling water) that are described in the following sections. The combination of both network formers (membrane C) resulted in nonbrittle, dimensionally stable transparent membranes.

Measurement techniques

FT-IR spectra were measured using a PerkinElmer 2000 FT-IR spectrometer in transmittance (precursors) and ATR modes (precursors, sols, gels, membranes). As the ATR crystal Ge or diamond was used. A horizontal ATR cell (Spectratech) and a Golden Gate single-reflection ATR cell (Specac) were used for detection of gelation and recording ATR spectra of the membranes, respectively. A Golden Gate heated diamond ATR top plate was connected to the temperature controller in order to perform in situ analysis of the membranes during heat-treatment from room temperature up to 433 K. The spectra were recorded at various temperatures during heating and cooling of the membranes inside a sample compartment that was continuously purged with dry nitrogen.

The proton conductivity of the membranes was measured in a "zero-gap"-type autoclave cell in the temperature range between room temperature and 433 K. The heating rate was 2° min^{-1} and the resistance at each temperature step was measured after at least 15 min of equilibration time. An HP 4284A LCR meter with Kelvin clamps and HP VEE OneLab software were used to measure resistance at 1 kHz alternating current. Thermogravimetric measurements of the membranes and precursors were made on a simultaneous differential scanning calorimetry (DSC)–thermogravimetric analysis SDT 2960 instrument from TA Instruments, Newcastle, USA, using a 10° min^{-1} temperature ramp under static air.

Table 1 Sol–gel processing of proton-conducting organically modified silanes

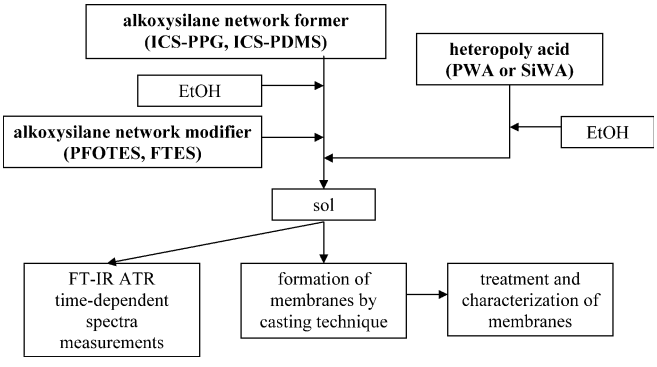

Results and discussion

Matrix formation and condensation

The sol–gel transition and further condensation of the material was followed in-situ in the IR spectrometer using an ATR horizontal cell with a Ge crystal as an internal reflecting element. The sol was placed on the crystal (dimensions 1 cm×7 cm) and the spectra were recorded at different stages of gelling and drying (Fig. 2). Dry gels obtained after 20 h contain a negligible

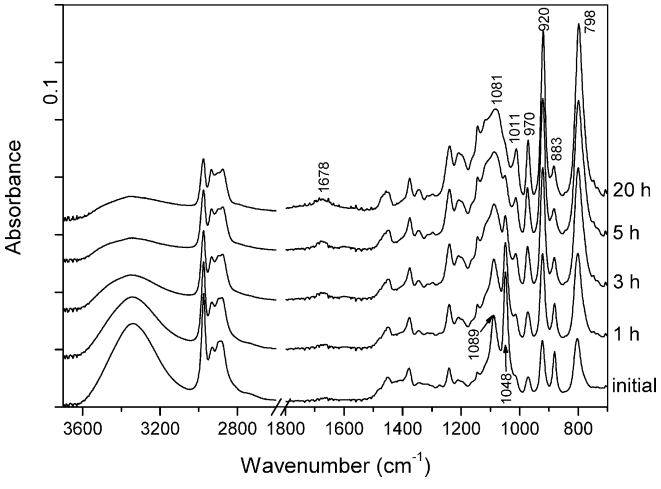

Fig. 2 Time-dependent IR attenuated total reflection (*ATR*) spectra of an ICS–PPG4000/PFOTES/SiWA/EtOH mixture

amount of the ethanol solvent. This was estimated from the intensity of the EtOH bands at 1,048 and 887 cm^{-1}; however, ethanol remained entrapped in the matrix for more than 10 h, as a consequence of the fast hydrolysis of the alkoxysilane precursors followed by immediate condensation because of the strong catalytic effect of SiWA. The condensation of the matrix is also observed from the small shift of the band at 1,089 cm^{-1} (initial spectrum) to lower wavenumbers (1,081 cm^{-1}, spectrum recorded after 20 h), characteristic of condensed Si–O–Si species. In the course of drying, as the sol becomes more concentrated owing to ethanol evaporation, the skeletal modes of the Keggin unit of SiWA (798, 883, 920, 970 and 1,011 cm^{-1}) also evolve, confirming the preservation of the Keggin ion structure inside the hybrid composite. These bands are relatively sharp and the strongest one is located at 798 cm^{-1}, indicating that the Keggin units are well-separated in the hybrid silica host, preventing strong anion–anion interactions [19, 20]. When the ICS–PDMS precursor is used as a network former, the Keggin ion bands at 798 and 1,011 cm^{-1} are blurred with the strong bands of the PDMS precursor itself at 800 and 1,024 cm^{-1}. In the spectral region of the amide bands (1,700–1,500 cm^{-1}), a single amide I band at 1,678 cm^{-1}, attributed to protonated carbonyls, developed after drying in both cases. The protonation of carbonyls with a strong HPA is characteristic [19, 20] and happens during the formation of a bulk gel from either ICS–PPG or ICS–PDMS network formers.

Thermal stability

Thermal analysis in an air flow was performed to evaluate the thermal stability of the ICS–PPG and ICS–PDMS precursors, as well as of some selected membranes derived from these precursors. We present here the results of thermogravimetric and DSC measurements of membranes A and B (Fig. 3) because the first was made from ICS–PPG, while membrane B consisted of ICS–PDMS. Membrane C represents a mixture of ICS–PPG and ICS–PDMS and its thermal behaviour with regard to DSC measurement (Fig. 3, dotted curve) lies between those exhibited by membranes A and B; however, membrane C represents the material of choice owing to its nonswelling properties and better thermal stability as compared with membrane A. In comparison with membrane B it is less thermally stable, but is not brittle like membrane B.

Fig. 3 shows that membrane B gradually lost mass, which we attributed to the loss of water as conceived from the temperature-dependent IR ATR spectra of the membrane (Fig. 4b). Despite the fact that IR ATR spectra were measured only up to 433 K, there was no reason not to attribute the loss of mass in the temperature interval up to 523 K to the release of water molecules incorporated in the membrane by the addition of the HPA. Conversely, membrane A showed a more

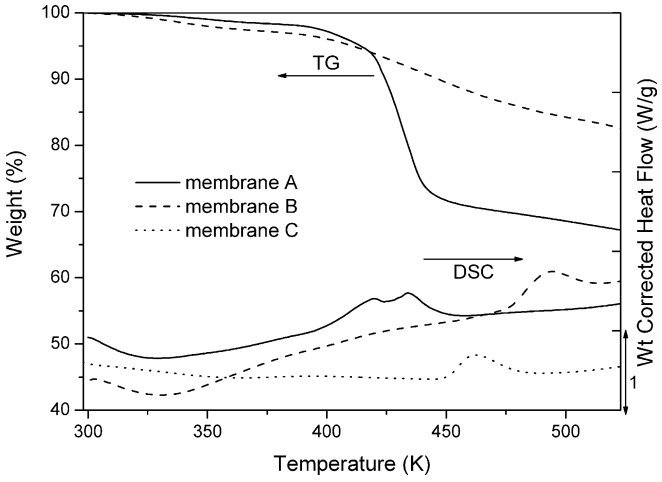

Fig. 3 Thermogravimetric (*TG*) and differential scanning calorimetry (*DSC*) curves of *membrane A*, *membrane B* and *membrane C*

pronounced mass loss, not exclusively attributed to the release of water molecules of SiWA. In the vicinity of 403 K the mass loss was accompanied by a heat flow, indicating structural changes of the sol–gel host. This we inferred from the IR ATR spectra (Fig. 4a) showing vibrational band changes in the 1,300–800-cm^{-1} region where skeletal modes of the ICS–PPG host appear [19]. We assume that these spectral changes are the consequence of organic polymer (PPG) destruction and conformational changes, since the material changes its colour and shape after heat treatment. The other two membranes, B and C, in contrast, did not show colour changes and kept their initial form. Like membrane B, also membrane C heated to 433 K did not show any substantial changes in the spectral range 1,300–800 cm^{-1} where the skeletal modes of the sol–gel host appear, confirming the stabilizing effect of the added ICS–PDMS to the less thermally stable ICS–PPG (Fig. 4c). Membrane C was thermally stable up to 448 K, exhibiting intermediate thermal stability with respect to membranes A and B, which was in agreement with its mixed precursor composition. At 448 K it started to deteriorate, showing an exothermic peak at 462 K (Fig. 3).

Owing to the complexity of the IR spectra of the membranes it was impossible to elucidate detailed information about the structural changes appearing during their heat treatment. These studies were left aside and the results of the IR spectral analysis will be published elsewhere.

Another thermal stability test, followed by IR ATR spectroscopy, involved treating the membranes in boiling water for 6 h to evaluate the extent of SiWA leaching. Using such an aggressive testing confirmed that ICS–PDMS membranes retained SiWA in their composite structure better than ICS–PPG membranes. This is not surprising owing to the more hydrophobic character of ICS–PDMS compared with ICS–PPG. As a result, the ICS–PDMS framework did not allow higher concentrations of HPA (above 40%), but this appeared to be enough to satisfy proton conductivities (see later).

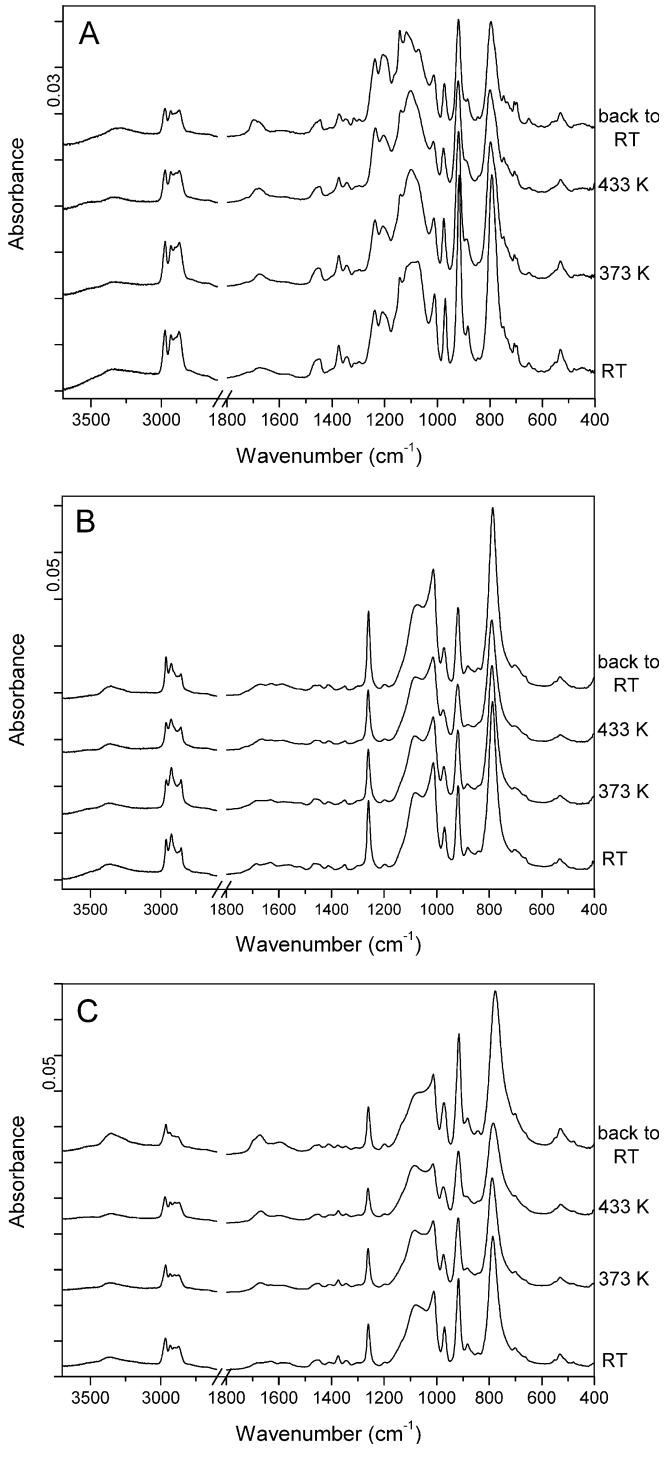

Fig. 4 Temperature-dependent IR ATR spectra of **a** membrane A, **b** membrane B and **c** membrane C. The spectra were recorded in situ at room temperature (*RT*), at 373 K, at 433 K and after cooling again to RT

Conductivity of the membranes

The mechanism of proton conduction in membranes used in PEMFCs operating at temperatures up to 353 K relies on the presence of water in the material. At low humidity and/or above the boiling point of water, the water content of the membrane decreases, leading to a decrease in cell performance due to the decrease of the conductivity of the membrane. The sol–gel membranes studied in this work belong to the class of membranes where water retention is enhanced owing to the presence of hydrophilic silsesquioxane units, assuring paths for the conduction of protons. The presence of urea groups linked to the PPG or PDMS connecting chains favours the establishment of additional channels for proton conduction. On the other hand, urea groups are sufficiently basic to dissolve and complex the HPA.

However, to attain a high water content in the membrane it is necessary to produce it from the amphiphilic molecules. In our membranes, the hydrophobic organic chains prevent excessive swelling at high temperatures and saturated humidity conditions, indirectly defining the conduction paths of the protons. We used PDMS or less hydrophobic PPG chains for this purpose. In this regard our membranes resemble a composite of Nafion/SiO_2–$2P_2O_5$–ZrO_2 and Nafion/SiO_2 + SiWA [24]. However, the results of the conductivity measurements on Nafion/gel and Nafion/particle composite membranes showed that the size of the hydrophilic clusters which influence the water content is not the only factor determining proton conductivity. It was stated that the structural changes induced by the insertion of hydrophilic clusters (gels or particles) play a decisive role in attaining proton conductivity and water retention at higher temperatures [25].

To demonstrate the beneficial effect of the amphiphilic structure of our membranes we performed conductivity measurements at saturated humidity conditions in the temperature interval 298–433 K. Since membranes B and C sustained temperatures up to 433 K, while membrane A showed degradation, we report here only the conductivity measurements on membranes B and C. We started with membrane C (previously treated in boiling water for 2 h), exposing it at 433 K for 18 h at saturated humidity conditions (Fig. 5). A steep increase in conductivity was noted during the first 2 h of autoclaving, indicating the relatively long stabilization time needed to attain a fully hydrated membrane. In the course of further autoclave treatment the conductivity increased only marginally.

In the next step we measured the temperature-dependent resistance of membrane C, as-prepared (untreated) and previously treated in boiling water for 2 h (Fig. 6). The temperature was gradually increased in intervals of 20 K starting at room temperature and finishing at 433 K. At each temperature the membrane was stabilized for 15 min before the temperature was increased again. The heating rate was only 2° min^{-1}, but was still not slow enough to assure equilibration of the water content in the membrane and therefore stable conductivity values. The conductivity gradually increased until 393 K was reached, where a sharp increase in conductivity was noted for the treated and untreated membranes. Above this temperature the

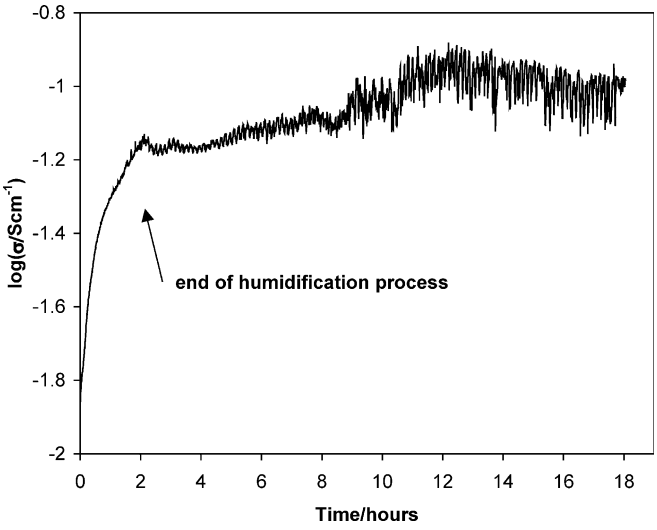

Fig. 5 Durability test of membrane C at 433 K and saturated humidity (conductivity versus time of exposure)

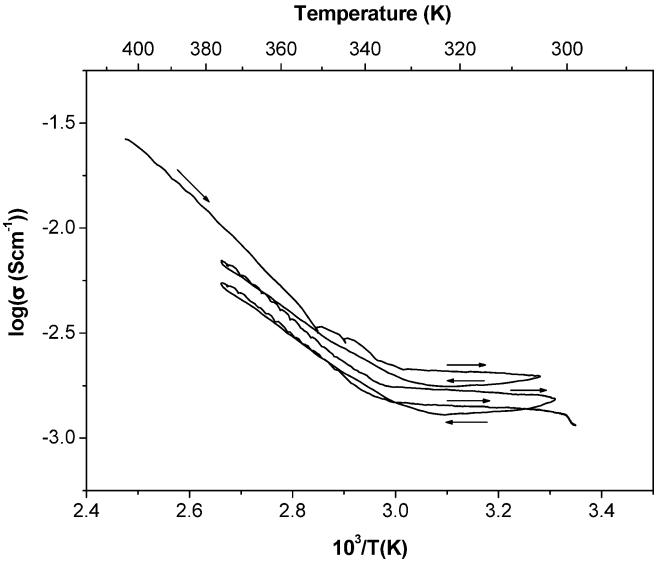

Fig. 7 Conductivity of membrane C at saturated humidity during temperature cycling

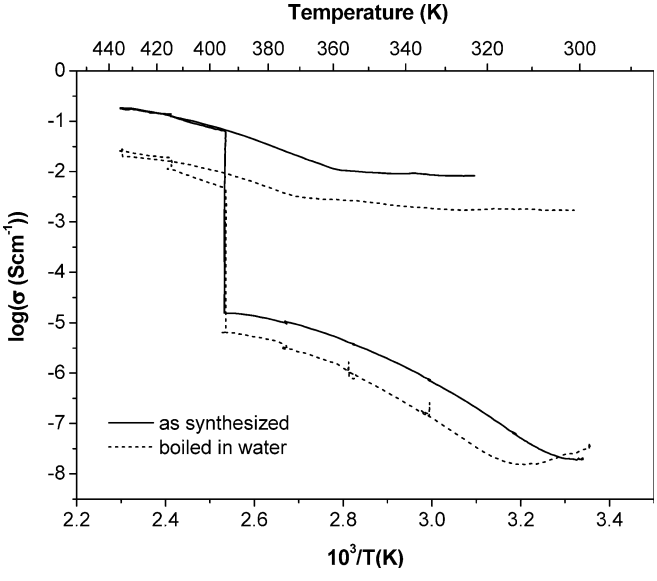

Fig. 6 Temperature-dependent conductivity of membrane C (as-synthesized and previously boiled in water) at saturated humidity

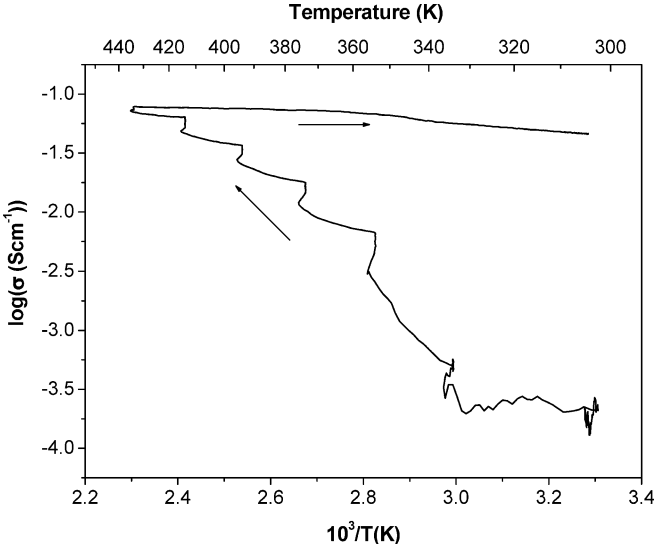

Fig. 8 Temperature-dependent conductivity of membrane B (as-synthesized) at saturated humidity

conductivity increased again but at a much lower rate. The highest conductivity at 433 K was approximately 3×10^{-2} and 2×10^{-1} S cm^{-1} for the previously treated and untreated membranes, respectively. During the cooling of the membrane back to the ambient temperature, a relatively small decrease in conductivity was observed. This was a consequence of humidification of the membrane, which was achieved during the heating process at saturated humidity and was not lost during the cooling process.

The stability of membrane C previously treated in boiling water was checked in the temperature interval 373–298 K (Fig. 7). Because of the conductivity jump noted at 393 K, before performing repetitive temperature cycling membrane C was heated to 403 K. Surpassing the conductivity threshold at 393 K shown in Fig. 6, we achieved a high conductivity of the membrane. The results showed that during three successive cooling/heating cycles in the lower-temperature range the conductivity did not change appreciably.

The temperature-dependent conductivity behaviour of membrane B was comparable to that of membrane C. Conductivities measured at various temperatures and 100% RH conditions in the temperature interval 298–433 K (Fig. 8) did not follow the same path as for membrane C, but the maximal conductivity was nearly the same. No drastic increase in conductivity was noted at a particular temperature, but it gradually increased.

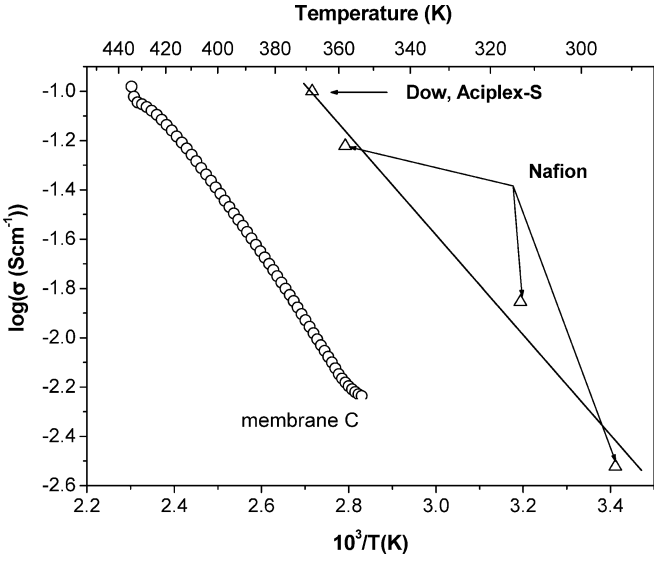

Fig. 9 Cooling branch of *membrane C* proton conductivity data in comparison with literature data on the conductivity of *Nafion*, *Aciplex-S* and *Dow* perfluorosulfonated membranes [26]

Finally, the activation energy was determined for membrane C from the Arrhenius plot shown in Fig. 9 (using the Arrhenius equation). The measurements were performed on a membrane 275-μm thick having a specific area resistance at 433 K (100% RH) of 0.275 and 4.89 Ω cm^2 at 353 K (100% RH). The activation energy at 100% RH was 20 kJ mol^{-1}, i.e. higher than that of Nafion (14 kJ mol^{-1}) [26] and Dow membrane (12 kJ mol^{-1}) [27] (Fig. 9).

Conclusions

Extensive studies of sol–gel-produced organic–inorganic composite gels comprising poly(propylene oxide) chains and PDMS chains grafted on silica particles by means of urea bridges revealed that ureasils doped with 12-tungstosilicic acids are promising materials for proton-conducting membranes. SiWA/ureasil membranes based on the combination of ICS–PDMS1000 (a precursor that combines the protonating ability of urea groups with the enhanced hydrophobicity of PDMS chains), ICS–PPG4000 and FTES silica precursors were found to exhibit high proton conductivity at temperatures above 363 K and saturated humidity, good thermal stability up to 423 K and excellent mechanical properties (toughness, no swelling in water). They are suitable candidates for application in PEMFCs at moderate temperature operating conditions.

Acknowledgements This work was performed under EU 5. FP project APOLLON, contract no. ENK5-CT-2001-00572.

References

1. Kreuer KD (2001) J Membr Sci 185:29
2. Rikukawa M, Sanui K (2000) Prog Polym Sci 25:1463
3. Kerres JA (2001) J Membr Sci 185:3
4. Jones DJ, Rozière J (2001) J Membr Sci 185:41
5. Bae J-M, Honma I, Murata M, Yamamoto T, Rikukawa M, Ogata N (2002) Solid State Ionics 147:189
6. Li L, Xu L, Wang Y (2003) Mater Lett 57:1406
7. Staiti P, Freni S, Hocevar S (1999) J Power Sources 79:250
8. Staiti P, Minutoli M, Hočevar S (2000) J Power Sources 90:231
9. Staiti P (2001) Mater Lett 47:241
10. Honma I, Nomura S, Nakajima H (2001) J Membr Sci 185:83
11. Nakajima H, Honma I (2002) Solid State Ionics 148:607
12. Honma I, Nakajima H, Nomura S (2002) Solid State Ionics 154–155:707
13. Honma I, Nakajima H, Nishikawa O, Sugimoto T, Nomura S (2002) Electrochemistry 70:920
14. Honma I, Nakajima H, Nishikawa O, Sugimoto T, Nomura S (2002) J Electrochem Soc 149:A1389
15. Nakajima H, Nomura S, Sugimoto T, Nishikawa S, Honma I (2002) J Electrochem Soc 149:A953
16. Honma I, Nakajima H, Nishikawa O, Sugimoto T, Nomura S (2003) J Electrochem Soc 150:A616
17. Honma I, Nakajima H, Nishikawa O, Sugimoto T, Nomura S (2003) Solid State Ionics 162:237
18. Wu Q, Tao S, Lin H, Meng G (2000) Mater Sci Eng B 68:161
19. Lavrenčič Štangar U, Grošelj N, Orel B, Colomban P (2000) Chem Mater 12:3745
20. Lavrencic Stangar U, Groselj N, Orel B, Schmitz A, Colomban P (2001) Solid State Ionics 145:109
21. Chang HY, Lin CW (2003) J Membr Sci 218:295
22. Tadanaga K, Yoshida H, Matsuda A, Minami T, Tatsumisago M (2003) Electrochem Commun 5:644
23. Dahmouche K, Atik M, Mello NC, Bonagamba TJ, Panepucci H, Aegerter MA, Judeinstein P (1997) J Sol–Gel Sci Technol 8:711
24. Damay F, Klein LC (2003) Solid State Ionics 162–163:261
25. Mauritz KA (1998) Mater Sci Eng C 6:121
26. Slade RCT, Varcoe JR (2001) Solid State Ionics 145:127
27. Halim J, Buchi FN, Hans O, Stamm M, Sherer GG (1994) Electrochim Acta 39:1303